www.dergipark.gov.tr
ISSN:2148-3736
El-Cezerî Fen ve Mühendislik Dergisi
Cilt: 9, No: 1, 2022 (189-202)

El-Cezerî Journal of Science and Engineering
Vol: 9, No: 1, 2022 (189-202)
DOI :10.31202/ecjse.956474

ECJSE

Research Paper / Makale

Investigation of the Effect of Movement Resistances on Battery Performance of a Passenger-Type Fuel Cell Vehicle Using Advisor Software

Mehmet Akif KUNT[1a*]

[1]Dumlupinar University, Department of Motor Vehicles and Transportation Technologies, Tavsanlı Vocational School, Dumlupinar University, Kutahya, TURKIYE
mehmetakif.kunt@dpu.edu.tr

Received/Geliş: 23.06.2021 **Accepted/Kabul:** 30.09.2021

Abstract: The most important factors affecting the performance of electric driven vehicles are battery technology and movement resistance. Although many researches have been made on vehicle performance of battery technologies, the number of researches on the effect of movement resistances (rolling resistance, air resistance, road gradient resistance, transmission resistance) and accessory losses on vehicle performance is quite limited. In this study, modelling of a passenger-type fuel cell vehicle has been made on ADVISOR (ADVISOR-Advanced Vehicle Simulator) simulation programme, and effect of movement resistances and accessory losses on battery performance has been examined. At the end of the simulation, it has been determined that $\boldsymbol{SOC}$ (State of Charge) value of the tire with low rolling resistance according to NEDC (New European Driving Cycle) driving cycle is higher than the tire with high rolling resistance by 2.2%; and that decrease of $\boldsymbol{C_xA}$ by two times has resulted in a decrease in $\boldsymbol{SOC}$ value by 1.3%. When vehicle-battery performance of transmission selection has been examined, it has been observed that higher friction loss occurred in 5-speed gearbox due to the differences between the gear rations of the gearbox, and average $\boldsymbol{SOC}$ value decreased by 1.4% due to the fact that accessory load was 1000 W instead of 700 W. During simulations made with relation to the incline of the road, usage of tire with low rolling resistance on road incline (ascend) of 5% resulted in a higher value of $\boldsymbol{SOC}$ by 2% and on road incline (descend) of 5%, usage of tire with low rolling resistance resulted in a higher value of $\boldsymbol{SOC}$ by 2.2%.

Keywords: Fuel cells, motion resistance, electrical vehicles, ADVISOR, State of Charge

Binek Tipi Yakıt Pilli Bir Aracın Hareket Dirençlerinin Batarya Performansına Etkisinin Advisor Yazılımı Kullanılarak İncelenmesi

Öz: Elektrik tahrikli araçların performanslarını etkileyen en önemli faktörler batarya teknolojileri ve hareket dirençleridir. Batarya teknolojilerinin araç performansına etkisi üzerinde çok miktarda araştırma yapılmasına rağmen hareket dirençleri (yuvarlanma direnci, hava direnci, yokuş direnci, transmisyon direnci) ve aksesuar kayıplarının araç performansına etkisi üzerine yapılan araştırma sayısı oldukça azdır. Bu çalışmada binek tipi yakıt hücreli bir aracın ADVISOR simülasyon programında modellemesi yapılarak hareket dirençleri ve aksesuar kayıplarının araç batarya performansına etkisi incelenmiştir. Simülasyon sonucunda NEDC sürüş çevrimine göre düşük yuvarlanma direncine sahip lastiğin SOC (State of Charge) değeri yüksek yuvarlanma dirençli lastikten % 2.2 daha yüksek, C_xA değerinin 2 kat azaltılması SOC değerinde % 1.3 azalma meydana getirmiştir. Transmisyon seçiminin taşıt batarya performansına bakıldığında vites kutusu dişli oranlarındaki farklılıklar sebebiyle 5 hızlı vites kutusunda daha yüksek sürtünme kayıpları meydana gelmiş, aksesuar yüklerinin 700 W yerine 1000 W olması ortalama SOC değerinin % 1.4 azalmasına neden olmuştur. Yolun eğimi ile ilgili yapılan simülasyonlarda % 5 yol eğiminde (yokuş) düşük yuvarlanma direncine sahip lastik kullanımı SOC değerinin % 2 daha yüksek elde edilmesini sağlamıştır. %5 yol eğiminde (iniş) ise düşük yuvarlanma direncine sahip lastik kullanılması durumunda SOC değeri % 2.2 daha yüksek elde edilmiştir.

Anahtar Kelimeler: Yakıt pilleri, hareket direnci, elektrikli araçlar, ADVISOR, State of Charge

How to cite this article
*Kunt, MA., "*Advisor-Based Modelling of a Passenger-Type Fuel Cell Vehicle and the Effect of Movement Tesistances on Battery Performance*" El-Cezerî Fen ve Mühendislik Dergisi 2022, 9 (1); 189-202.*

Bu makaleye atıf yapmak için
*Kunt, MA., "*Binek Tipi Yakıt Pilli Bir Aracın Hareket Dirençlerinin Batarya Performansına Etkisinin Advisor Yazılımı Kullanılarak İncelenmesi*"* El-Cezerî Fen ve Mühendislik Dergisi 2022, 9 (1); 189-202.
ORCID ID: [a]0000-0001-5710-7253

1. Introduction

The demand for environment friendly vehicles increases day by day throughout the world due to emission standards. Electric and fuel cell vehicles are among the most important environment friendly vehicle alternatives thanks to their capabilities of high efficiency, silent functioning and low emission production. Fuel cell is a system generating electrical power using a suitable fuel and oxidant and creating electro-chemical reactions. Fuel and the oxidant react in an electrolyte environment. In fuel cells, the ones that will react enter into the cell, reaction products leave the cell and electrolyte remains in the cell. In the event that the suitable fuel and the oxidant feed the fuel cell constantly, the fuel cells can run forever in terms of duration. As ranges of the vehicles that are completely electrical are short, and due to long period of charging and storage problems, their speed of proliferation is low. One of the solutions for energy storage problem in electric vehicles is fuel cell practice [1]. In vehicles driven by electrical power, basic energy losses include energy storage systems, electrical engine, power transmission elements, gradient resistance, air resistance, rolling resistance and acceleration resistance [2]. The factors, which should be considered in order to increase ranges of electrical vehicles, are front vehicle projection area, battery power density and rolling resistance coefficient [3]. Apart from such factors, the road gradient is one of the most important factors affecting the energy consumption and ranges of electrical vehicles [4-6]. While studies on battery technologies and regenerative recovery technologies aiming to increase ranges of completely electrical, hybrid-electrical and fuel cell vehicles are high in number [7-8]; the number of studies on decreasing movement resistances of vehicles is less. In this study, effects of parameters of rolling resistance, air resistance, gradient resistance, transmission and accessory load on battery performance by means of modelling a passenger-type fuel cell automobile using the ADVISOR vehicle simulation programme.

1.1 Capabilities of ADVISOR Software

The fuel cell model prepares should have a physical and mathematical meaning [9]. Unless such two requirements are met, the level of reliability on obtained results remains low. After composing the foundation of the model, its scope should be formed delicately.

Figure 1. ADVISOR block diagram

The simulation software ADVISOR used is an open source software and can be used offline. In order to make modelling and simulation in ADVISOR, Matlab Simulink module is used. ADVISOR simulation program is an interface program that works integrated with Matlab Simulink program to perform all kinds of vehicle simulations and does not work independently of Matlab Simulink (Figure 1). One of the advantages of using Matlab Simulink interface is its provision of convenience for making changes on ADVISOR vehicle model, control strategy and algorithm [10]. This programme establishes a relation between the power source of the vehicle and the wheels. Moreover, the programme authorities have made agreements with certain commercial automobile manufacturers and used the algorithms included in the industry and minimized the uncertainties of the programme. Another advantage of this programme is the fact that the user can make selection among the 9-defined driving system and 19 engines, 9 batteries and 7 fuel cell functioning by electricity during the modelling [11]. The ADVISOR block diagram is shown in Figure 2.

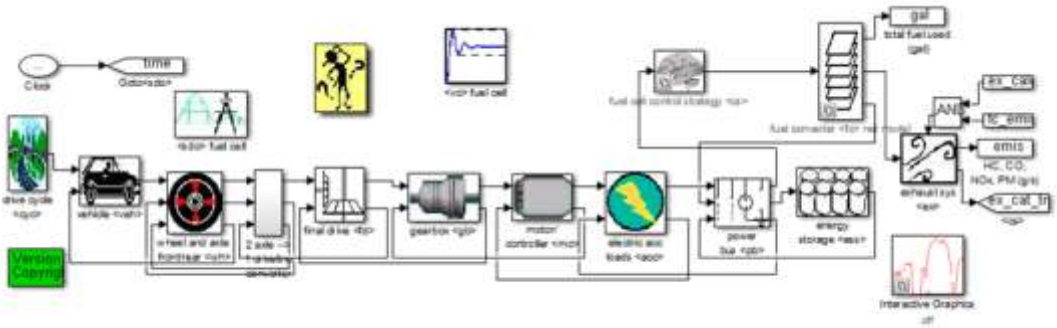

Figure 2. ADVISOR block diagram

2. Modelling of the Vehicle

Forces affecting the movement of the vehicle can be classified into two groups as resistance forces and traction forces [12]. Resistance forces are rolling resistance (F_r) aerodynamic resistance (F_w), inertial resistance that the vehicle should exceed (F_a) and inclination resistance (F_{st}) on vehicles as given in equation 1. In figure 3, forces acting on the vehicle are shown [13]. In Table 1, force parameters from which the vehicle is affected are given.

$$F_t = F_r + F_w + F_a + F_{st} \tag{1}$$

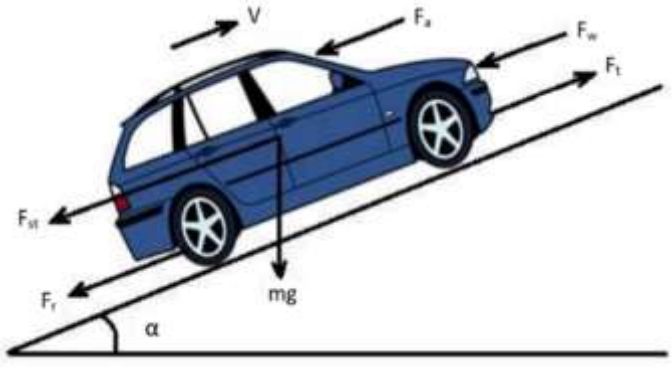

Figure 3. Forces affecting the vehicle

$$F_r = c_{r,ro} mg + c_{r,r1} mgV \tag{2}$$

In equation no (2), $c_{r,ro}$, $c_{r,r1}$ indicate 1st and 2 nd rolling resistance coefficients, "m" indicates the vehicle mass, "g" indicates gravity acceleration and "V" indicates vehicle speed.

$$F_w = \frac{1}{2}\rho C_d A_f V^2 \quad (3)$$

In equation no (3), "ρ" indicates air density, "C_d" indicates aerodynamic friction coefficient, "A_f" indicates frontal cross-sectional area.

$$F_a = mM_i \frac{dV}{dt} \quad (4)$$

In equation no (4), "M_i" indicates rotational inertial mass constant, $\frac{dV}{dt}$ indicates vehicle acceleration.

$$F_{st} = mg \sin \alpha \quad (5)$$

In equation no (5), "α" indicates the elevation of the road [14].

Batarya SOC;

$$SOC\ (t) = SOC\ (t-1) + \int_0^t \frac{I}{C_{bat}} dt \quad (6)$$

In equation no (6), "t" indicates time (h), "I" charge/discharge current (A), indicates "C_{bat}" battery capacity (Ah) [2].

3. Material and Method

Parameters of the electrical vehicle which was modelled are shown in Table 1. The result graphics have been composed by means of ADVISOR vehicle simulation programme. As fuel cell vehicles are more efficient during intra-city driving, the NEDC (New European Driving Cycle) driving cycle, whose acceleration/slowing number is more than the other driving cycles, has been used. It has been accepted that the vehicle moves within stagnant-air and wheel pressure and load affecting the wheel vertically do not change during the drive.

Table 1. Model parameters of the vehicle

Data	Values	Units
Vehicle mass	1573	kg
Wheel diameter	0.35	m
Gravitational acceleration	9.81	m/s^2
Air density	1.204	kg/m^3
Differential gear ratio	10	%
Electric motor	MCAC75	
Electric motor efficiency	90	%
Electric motor max. current	1000	A
Electric motor min. voltage	60	V
Wheel size	205/60 R15	
Battery type	Nimh	
Battery efficiency	95	%
Number of battery modules	40	
Battery capacity (for 1 module)	6.5	Ah

While examining the effect of rolling resistance on vehicle performance, calculation relations used under SAE J2452 standards have been used. While examining the effect of road gradient on vehicle performance, battery performance graphics have been formed according to road ascend of ±%5.

While examining the effect of aerodynamic resistance on vehicle performance, the battery performance have been analyzed according to 4 different C_xA values included in the literature. While examining the effect of transmission on vehicle performance, 1-speed and 5-speed transmission options have been taken into consideration. While examining the effect of accessory loads, analyses have been made in consideration with the energy consumption of an average passenger-type automobile.

4. Results and Discussion

4.1. Rolling Resistance

Factors resulting in energy loss on the vehicle are named as resistance forces. The most important one of these forces is the rolling resistance [15]. SAE J2452 wheel standard, differently from the previously used SAE J1269 standard, determines the rolling resistance force as a function of vehicle load, wheel pressure and speed, instead of accepting the steady wheel functioning conditions. According to SAE J2452 wheel standard, the rolling resistance force is as follows:

$$F_r = P^{\alpha} Z^{\beta} (a + bV + cV^2) \quad (6)$$

In relation no (1), (P) represents the wheel pressure, (Z) represents the load affecting the wheel vertically, (a, b, c) represent the calculation coefficients. Values of (a), (b) and (c) coefficients have been shown in Table 2 respectively according to the rolling resistance.

Table 2. Rolling resistance force calculation parameters as SAE J242 test standards [16].

	a	b	c
Rolling resistance (low)	0.0682	$2.32*10^{(-4)}$	$1.2 * 10^{(-6)}$
Rolling resistance (high)	0.159	$3.44*10^{(-4)}$	$1.25 * 10^{(-6)}$

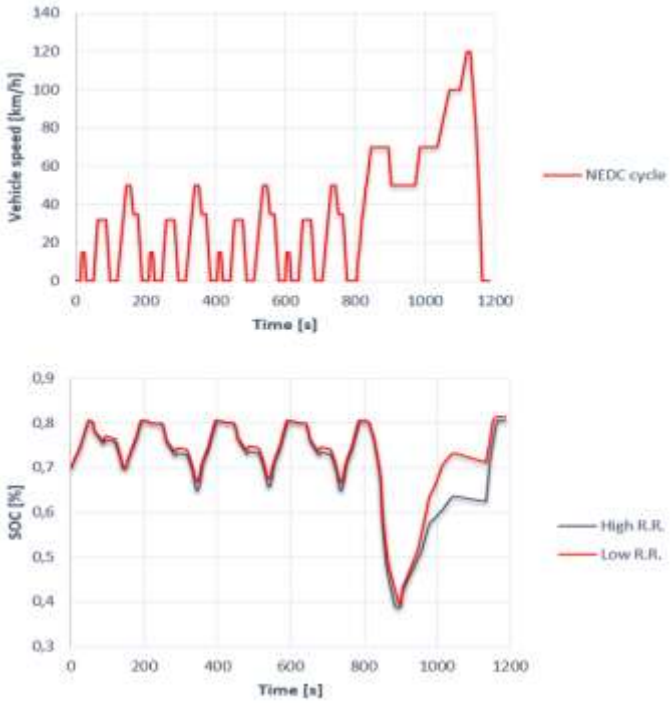

Figure 4. Graphic of SOC change according to time

In Figure 4, graphic of SOC change has been shown according to time. SOC charging level has been accepted as 70% in the beginning of the simulation. SOC maximum value is 80%, minimum value is 40%. Accordingly, during the driving cycle, regenerative recovery has been maintained in 11 different points. In driving cycle, SOC level only decreased at the 900th second for both wheel types by 40%; after that point, the recovery system increased the charge level up to 80% until 1170th second. In case of usage of wheel with low rolling resistance, more recovery energy has been obtained during deceleration. According to driving cycle 1, average SOC value has been obtained as 70.2% in Wheel with high rolling resistance, and as 72.2% in wheel with low rolling resistance. Moreover, the increase in vehicle speed and frequency of speed change has increased the difference between SOC values of wheels with low and high Rolling resistance (time interval between 900-1170 seconds).

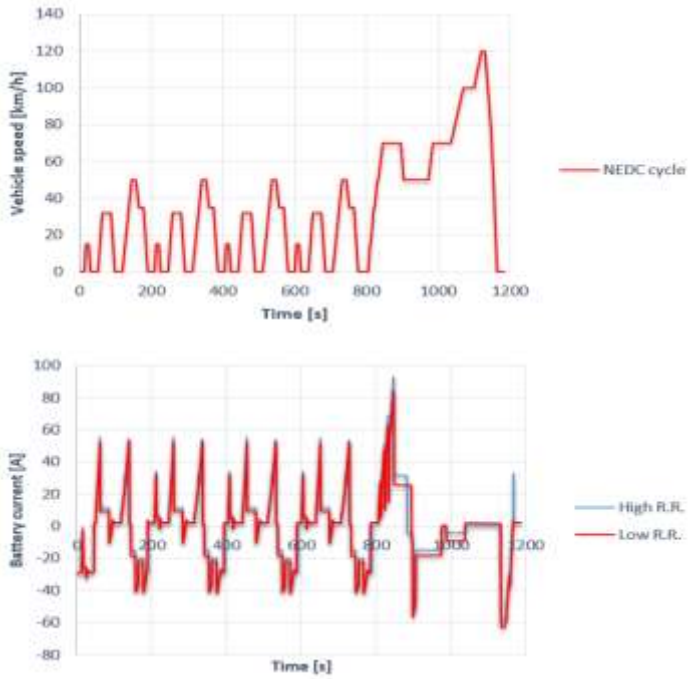

Figure 5. Graphic of time-dependent battery current change

In Figure 5, Graphic of time-dependent battery current change has been shown. The starting point of the graphic is the negative current area due to regeneration. During all acceleration processes, due to power transfer organs, electrical engine of the vehicle, the inertia in the batteries and resistance forces, the current driven from the battery increased fast and then it decreased a bit. During the driving cycle, wheels with high rolling resistance draw much more current from the batteries. In the cycle graphic, the effect of the change in rolling resistance force after the 800th second can be seen clearly. In this simulation study, the energy spent by wheels with low and high rolling resistance during rolling, braking loss energy, fuel consumption and equivalent oil consumption have been calculated. The values of related parameters are shown in Table 3.

Table 3. Effect of rolling resistance coefficients on rolling, braking and fuel consumption

	Rolling energy (kJ)	Brake loss (kJ)	H_2Fuel consumption(l/100km)	Gasoline equivalent (l/100km)
High R.R.	1843.6	580.69	60.9	4.1
Low R.R.	952.51	629.92	55.1	3.7
	48.3%	7.8%	9.5%	9.75%

According to Table 3, the energy spent by the wheel with high rolling resistance is higher by 48.3%. In the Wheel with high rolling resistance, the energy spent during braking is less by 7.8% and H_2 fuel consumption of the wheel is higher by 9.5%. Additionally, when equivalent oil consumption is observed, it is seen that in case of usage of Wheel with low rolling resistance, the fuel consumption decreases by 9.75%.

4.2. Road Gradient

Road gradient is one of the basic factors affecting the vehicle's fuel economy [17]. Vehicles driven by electrical energy are affected less from the road gradient when compared to internal combustion engines with fossil fuel [18-20]. The basic reason of such situation includes the torque characteristics of the electrical engines and low level of transmission losses. Road gradient is generally ignored in studies related to vehicle's fuel economy and performance. Such situation causes significant calculation mistakes during vehicle performance evaluation [21]. In Figure 6, time-dependent SOC change on road gradient of 5% has been shown. During climbing of the vehicle, gradient resistance is added into air resistance, rolling resistance and acceleration resistance. Usage of wheel with high rolling resistance has caused energy consumption to increase. Such situation generally increases the energy consumption of the vehicle and causes batteries to require more frequent and long term regenerative braking. According to the simulation, in road gradient of 5% (incline), if wheel with high rolling resistance is used, the average SOC value for driving cycle 1 has been calculated as 64.2%; if Wheel with low rolling resistance is used, the average SOC value has been calculated as 66.2%.

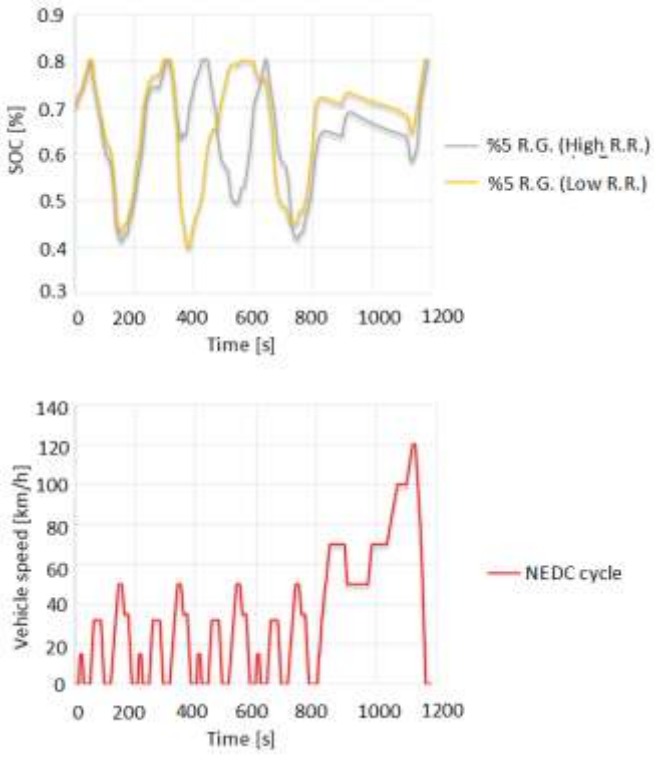

Figure 6. Time dependent SOC change graphic for road gradient of 5% (decline)

In Figure 7, Time dependent SOC change graphic for road ascend of 5% (decline) has been shown. During decline of the vehicle, while air resistance, rolling resistance and acceleration resistance decrease the kinetic energy of the vehicle, ascend of the road increases the kinetic energy of the road. Increase of energy consumption in the wheel with high rolling resistance, when compared to the wheel with low rolling resistance, has resulted in decrease of the recovery amount. As road gradient is downside, batteries are charged more frequently and for short terms. Usage of

regenerative braking system has resulted in less need for the braking system of the vehicle. Such situation increases the lifetime of brake lining. According to the simulation, in road ascend of 5% (incline), if wheel with high rolling resistance is used, the average SOC value for driving cycle 1 has been calculated as 78.2%; if wheel with low rolling resistance is used, the average SOC value has been calculated as 80.4%.

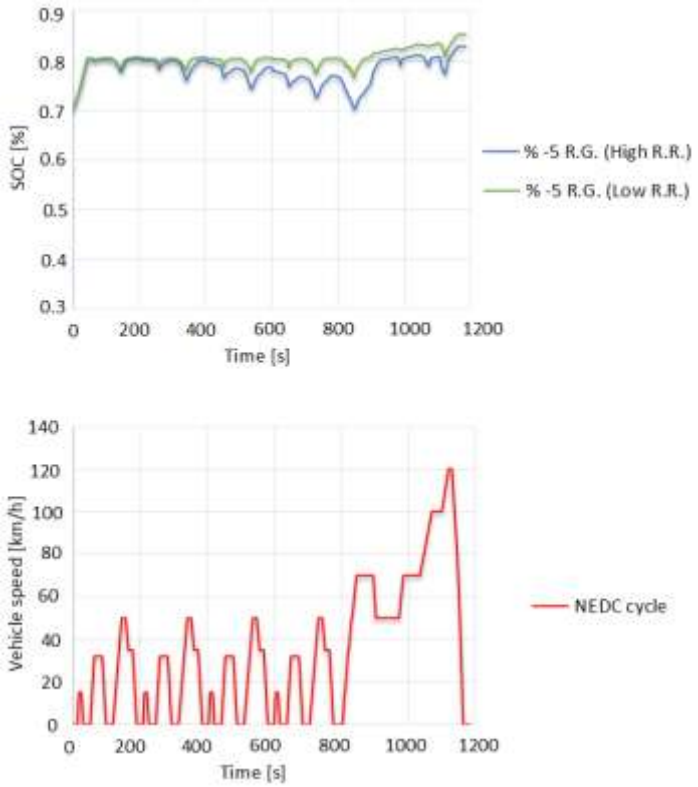

Figure 7. Time dependent SOC change graphic for road ascend of 5% (decline)

4.3. Aerodynamic Drag

Aerodynamic resistance force is one of the most important resistance forces affecting the vehicle during motion. Aerodynamic resistance force changes the vehicle's driving power of the vehicle [22]. Aerodynamic resistance of the vehicle can be decreased by regulating the front projection area and aerodynamic resistance coefficient. 50% of the aerodynamic resistance exposed by a typical passenger type automobile is composed of upper body of the vehicle; 25% of Wheel and shroud area and 25% due to the effect of air flowing under the vehicle [23]. In electrical vehicles, the battery groups are placed in front and rear axles, differently from traditional automobiles, and they improve the balance, usage and driving of the vehicle. Making the centre of gravity of the vehicle approach to the ground increases aerodynamic performance. In passenger-type automobiles, front bumper [24-25], windshield inclination [26], ceiling inclination [27-28], rear bumper [29-30], bottom casing [31-33], wheels and side mirror designs are all effective on aerodynamic resistance coefficient (C_x). Bu changing (C_x) aerodynamic resistance coefficient and (A) characteristic projection area, 4 different front sections have been obtained. The obtained front section area includes the vehicle front section area data used in the literature [34]. Moreover, assuming that the vehicle moves within still air, the speed of wind was disregarded. It was assumed that the Rolling resistance have not changed and there is no road ascend. In Figure 8, time dependent vehicle power consumption change in driving cycle 1 is shown. As speed changes between time interval of 0-800 s of the driving cycle, similar consumptions have been obtained for different C_xA values during power consumption. Between the time interval of 800-1200 s, power consumption of the vehicle

has become more evident. In terms of average of the power consumption of the cycles, it was seen that the design with the highest C_xA value has the highest power consumption rate. For values of C_xA=0.39, 0.58, 0.68 and 0.78 respectively, power consumption of 780 W, 1163 W, 1365.2 W and 1582.53 W has occurred. Reducing the C_xA by two times causes a decrease in vehicle power consumption by a rate of 50.7%.

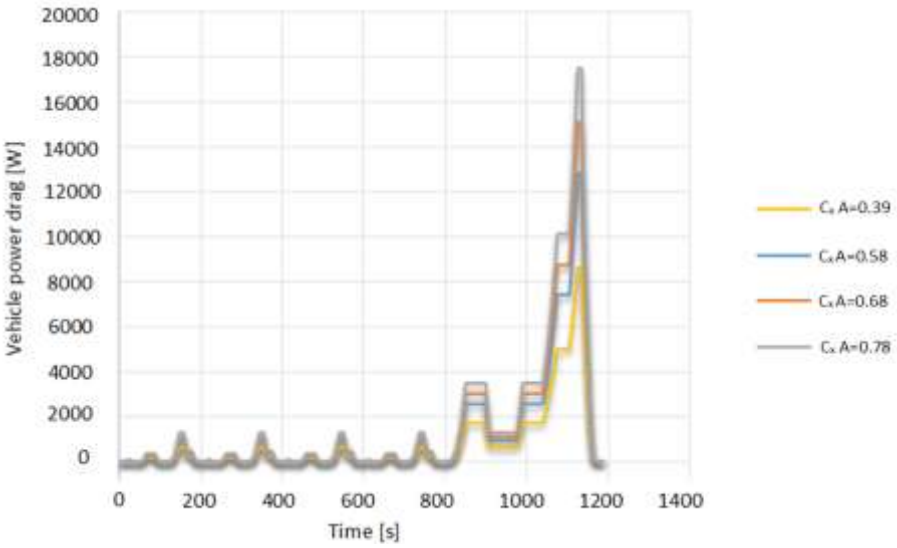

Figure 8. Graphic of time dependent power consumption

In Figure 9, time dependent SOC change has been shown. The value of SOC in the beginning of the cycle has been considered as 70%. As speed changes between time interval of 0-800 s of the driving cycle is less, similar SOC values have been obtained for 4 different C_xA values. After the 800th second, the highest speed change has been obtained in driving cycle and during such change the SOC value of the battery obtained the lowest level. After that point, regeneration has been provided and a higher charging value has been obtained in the design with C_xA=0.39 value. The reason of such situation is the fact that designs with low C_xA value requires more braking energy. As regeneration energy has been obtained partly from braking energy, higher recovery has been obtained. In the simulation study carried out, for values of C_xA=0.39, 0.58, 0.68 and 0.78 respectively, SOC values of % 72.3, % 71.8, %71.5 and % 71 have occurred. Reducing the C_xA by two times causes a decrease in SOC value by a rate of 1.3%.

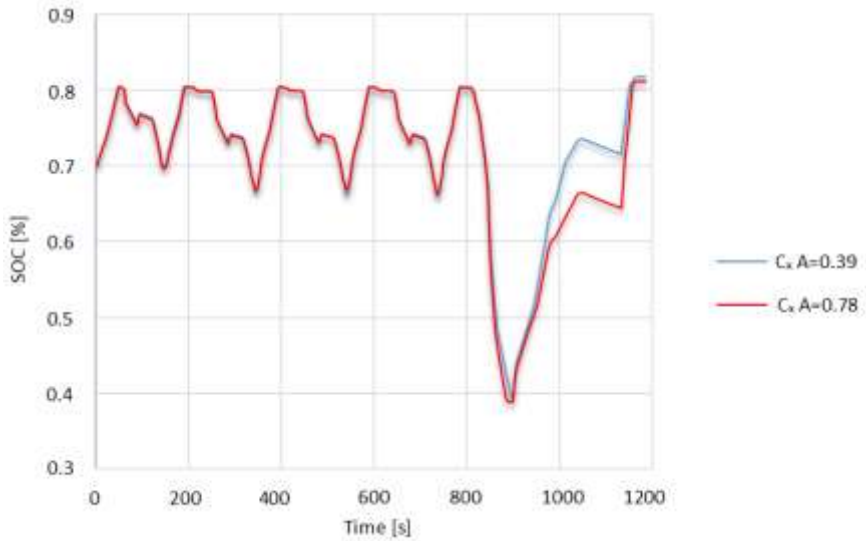

Figure 9. Time dependent SOC change graphic

4.4. Transmission

In Figure 10, effect of usage of transmissions with 1 and 5 speed on SOC change is shown. Gear ratio of gearbox with 1-speed is 6.67; gear rate of the gearbox with 5-speed is 13.45. In the time interval between 0-800 seconds, SOC changes of both gearboxes are highly close to each other. In the time interval between 800-1200 seconds, speed change has been obtained between vehicle speeds of 50 km/h-120 km/h. In such time interval, SOC level of 5-speed gearbox decreased to 0.1 value. In high vehicle speeds, 5-speed gearbox created much mechanical loss and reduced SOC level to 0.1 value.

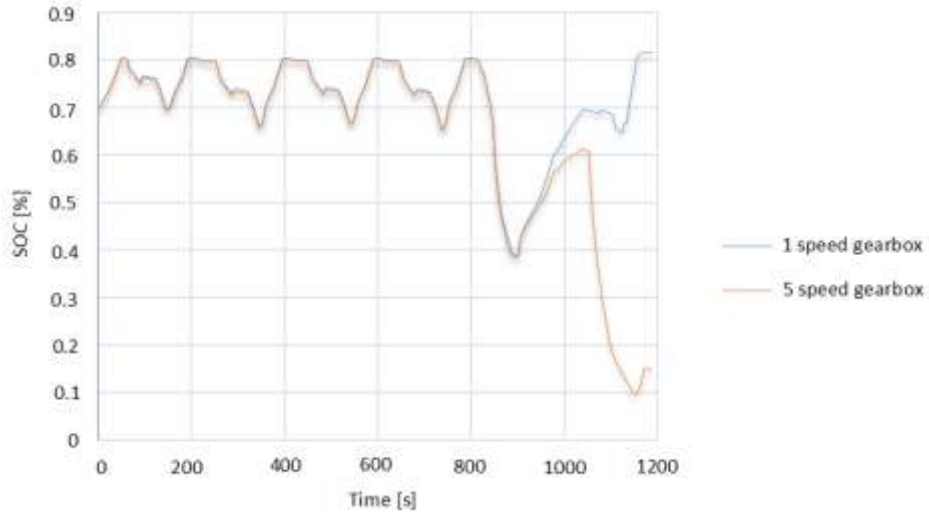

Figure 10. Time dependent SOC change graphic for different transmission usages

In Figure 11, gearbox outlet torque change is shown for transmission usages with 1 and 5 speeds. 5-speed gearbox has obtained higher gearbox outlet torque during the driving cycle. Especially in the time interval between 800-1200 seconds, although power need of the vehicle increased, vehicle power consumption increased as gearbox generated high outlet torque. In the time interval between 800-1200 seconds, gearbox with 1-speed provided 93.92 Nm outlet torque, and 5-speed gearbox provided 320.47 Nm outlet torque. In such interval, mechanical frictions of the gearbox with high gear ratio occurred much more.

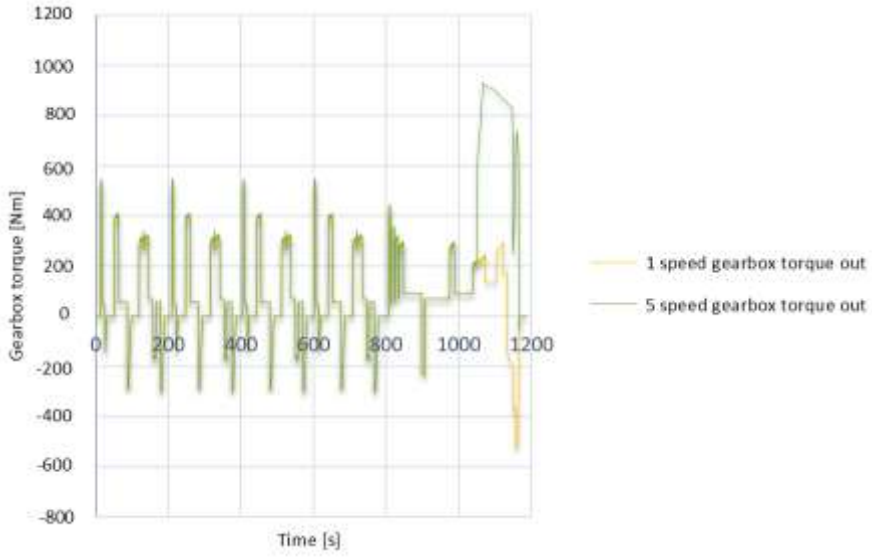

Figure 11. Time dependent gearbox outlet torque change for different transmission usages

In Figure 12, time dependent fuel consumption change of transmission usages with 1 and 5 speed is shown. In the intervals of the cycle where speed change of 0-50 km/h occurred, fuel consumption changes of both gearboxes showed similarity; in the intervals where speed changes occur between 50-120 km/h, fuel consumption changes took different values. In the time interval between 800-1200 seconds, in the vehicle with 5-speed gearbox with high gear rate, avarage fuel consumption flow was 0.94 g/s, while in the vehicle with 1-speed gearbox such figure is 0.92 g/s. In the related time interval, usage of 1-speed gearbox provides a saving of 2.1% with respect to fuel consumption.

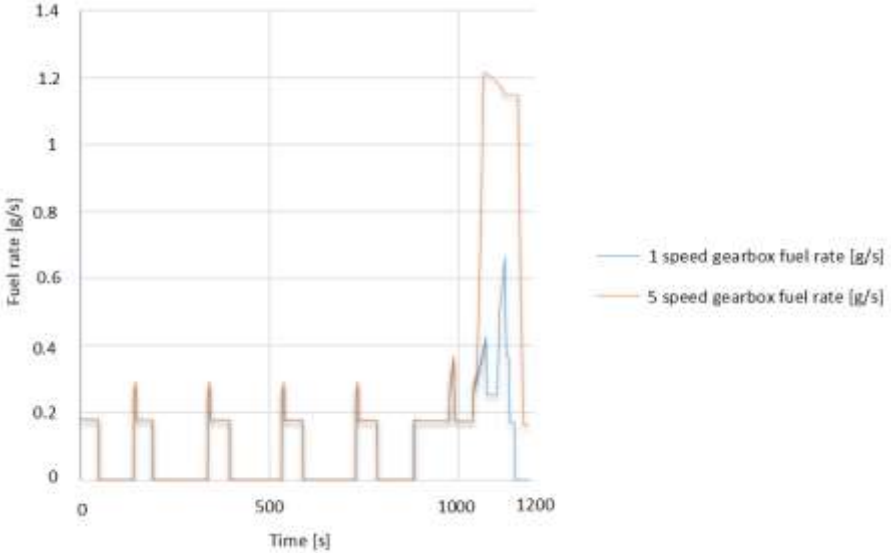

Figure 12. Time dependent fuel consumption for different transmission usages

4.5. Accessories

The energy driven by accessory loads is almost equal to the energy required for movement of the vehicle [35-36]. During driving process, A/C, electro-hydraulic steering Wheel and electrical receivers consume energy from the batteries according to road, load and climate conditions.

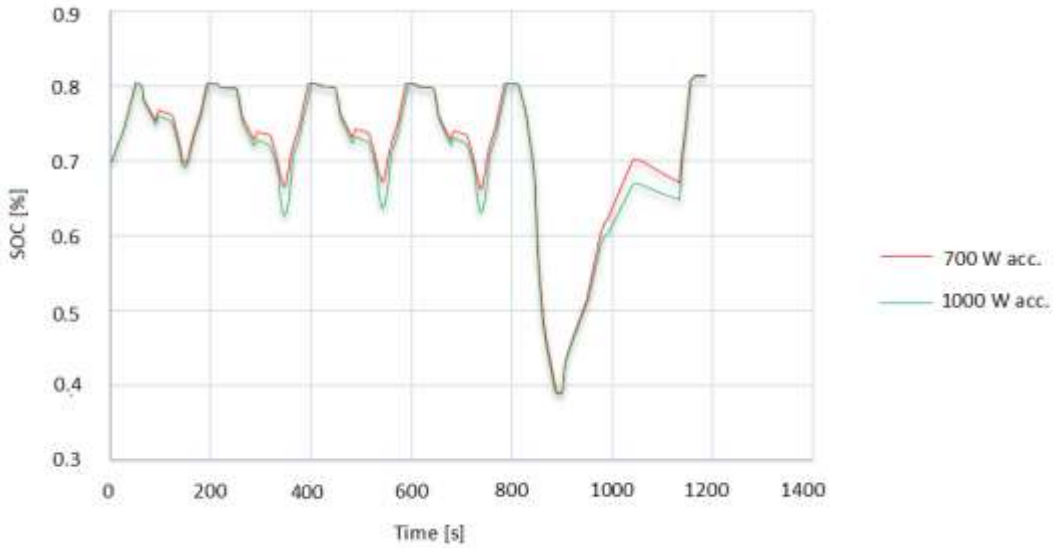

Figure 13. Time dependent SOC change for different accessory loads

In Figure 13, SOC change graphic for accessory loads of a passenger type vehicle is seen. In the time interval between 0-800 seconds, speed changes between 0-50 km/h. In this time interval, an average charging level of 75.4% has been obtained in the vehicle with 700 W accessory load; and an average charging level of 74.4% has been obtained in the vehicle with 1000 W accessory load. In

the time interval between 800-1200 seconds, speed changes between 0-120 km/h. Increase of total resistance in speeds between 0-120 km/h has clarified the SOC difference between the vehicles having accessory loads of 700W and 1000W. In the time interval between 800-1200 seconds, an average charging level of 63.6% has been obtained in the vehicle with accessory load of 700 W; and an average charging level of 62.2% has been obtained in the vehicle with accessory load of 1000 W.

In Figure 14, effect of accessory load and accessory efficiency is shown. As the speed changes in driving cycle are linear, a linear trend has occurred in the graphics. Reduction of accessory load and usage of electrical receivers with high efficiency have decreased fuel consumption. On the other hand, increase of electrical power consumption or usage of electrical receiver with low efficiency increase fuel consumption.

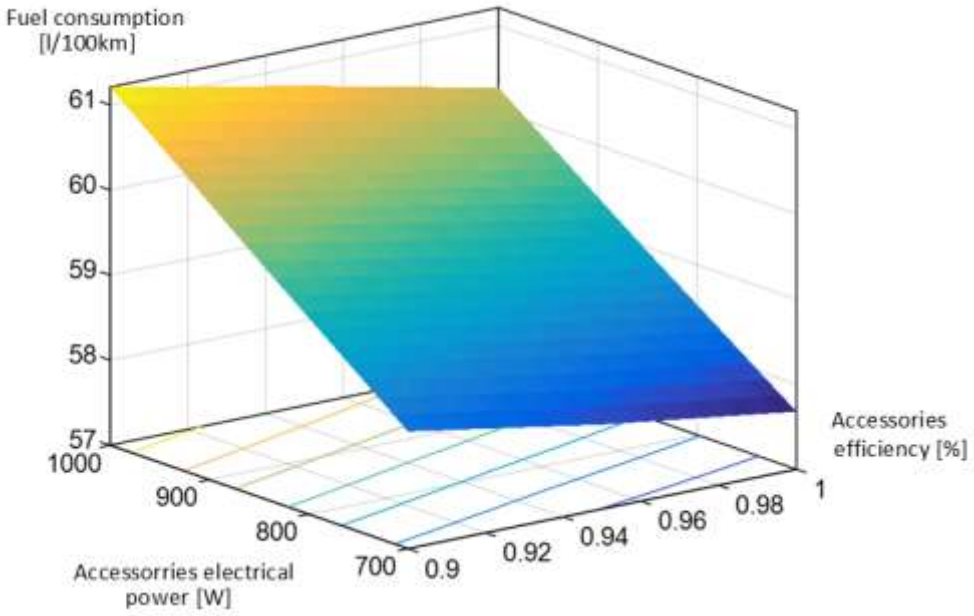

Figure 14. Effect of accessory load and efficiency on fuel consumption

5. Conclusions

In this study, effect of vehicle motion resistances on a passenger type automobile using fuel cell has examined. In case of usage of wheel with loss rolling resistance, higher recovery energy is obtained during slowing down. During the driving cycle, wheels with high rolling resistance withdraw high current from the batteries. In the simulations carried out with relation to road ascend, in the road gradient of 5% (incline), usage of wheel with low rolling resistance resulted in increase in SOC value by a rate of 2%. When the road ascend is downside, batteries are charged more frequently. Therefore, SOC value of the Wheel with low rolling resistance is higher than the wheel with high rolling resistance by a ratio of 2.2%. Decrease of C_xA value caused a decrease in SOC value. When vehicle battery performance of transmission selection is considered, much friction loss occurred in 5-speed gearbox due to differences in gear ratio. Such situation increased fuel consumption. Increase of accessory losses resulted in low SOC values especially in high speeds. High efficiency of electrical receivers of the vehicle decreases fuel consumption.

Yazarların Katkıları

MAK makaledeki analiz ve çalışmalarını yürüttü, makale yazımını yaptı. Makalenin son halini okudu ve onayladı.

Çıkar Çatışması

Yazar, çıkar çatışması olmadığını beyan eder.

References

[1]. Pehnt, M., Life-cycle Assessment of Fuel Cell Stacks, Hydrogen Energy, 2001, 26(10): 91–101.

[2]. Kunt M. A., "Tümüyle Elektrikli Binek Tipli Bir Aracın ADVISOR Tabanlı Modellenmesi ve Aerodinamik Direnç Değişiminin Batarya Performansına Etkisi Üzerine Bir Çalışma", The 1st Internatıonal Symposium on Automotive Science and Technology (ISASTECH2019), Ankara, 5-6 September 2019.

[3]. Yuan, X., Li, L., Gou, H., Dong, T., Energy and Environmental Impact of Battery Electric Vehicle Range in China, Applied Energy, 2015, 157: 75-84.

[4]. Cicero-Fernândez, P., Long, J. R., Winer A. M., Effects of Grades and Other Loads on On-Road Emissions of Hydrocarbons and Carbon monoxide, J. Air Waste Manage. Assoc., 1997, 47: 898–904.

[5]. Zhang, K. S., Frey, H. C., Road Grade Estimation for On-Road Vehicle Emissions Modelling Using Light Detection and Ranging Data, J. Air Waste Manage. Assoc., 2006, 56: 777–788.

[6]. Boroujeni, B.Y., Frey, H. C., Sandhu, G. S., Road Grade Measurement Using In-Vehicle, Stand-Alone GPS with Barometric Altimeter, J. Transp. Eng., 2013, 139: 605–611.

[7] Kunt, M. A., Advisor Based Modelling of Regenerative Braking Performance of Electric Vehicles at Different Road Slopes, Internatıonal Journal of Automotıve Science and Technology, 2020, 4: 98-104.

[8] Kunt, M. A., A study on the Effect of Rolling Resistance Change on Acceleration Performance and Transmission Losses in An All-Electric Passenger Type Vehicle, El-Cezerî Journal of Science and Engineering, 2020, 7: 743-752.

[9]. Türkmen, A. C, Solmaz, S., Cenk, C., Analysis of Fuel Cell Vehicles with ADVISOR Software, Renewable and Sustainable Energy Reviews, 2017, 70: 1066–1071.

[10]. Markel, T., Wipke, K., Haraldsson, K., Kely, K., Vlahinos, A., Fuel Cell Vehicle Systems Analysis, Hydrogen, Fuel Cells and Infrastructure Technologies Annual Program Review, 2003.

[11]. Zhou Y. L., "Modeling and Simulation of Hybrid Electric Vehicles", Yüksek lisans tezi, University of Science & Tech. Beijing, 2005.

[12]. Zhang, Y., Zhang, C.," ADVISOR and Its Application in Electric Vehicle Simulation", Proceedings of the 30th Chinese Control Conference, (2011).

[13]. Suvak, H., Erşan, K., The Simulation of a Full Electric Vehicle Using the City Cycle, International Journal of Automotive Engineering and Technologies, 2017, 5(2): 38-46.

[14]. Boisvert, M., Mammosser, D., Micheau, P., Desrochers, A., Comparison of Two Strategies for Optimal Regenerative Braking, with Their Sensitivity to Variations in Mass, Slope and Road Condition, IFAC Proceedings, 2013, 46(21): 626-630.

[15]. SAE Standartları Testleri. (2019). <https://www.eurolab.com.tr/sektorel-test-ve-analizler/endustriyel-testler/sae-standartlari-testleri>.

[16]. Kunt, M. A., "Tümüyle Elektrikli Binek Tipli Bir Araçta Yuvarlanma Direnci Değişiminin İvmelenme Performansı ve Transmisyon Kayıplarına Etkisi Üzerine Bir Çalışma", The International Conference of Materials and Engineering Technology (TICMET'19), Gaziantep, Türkiye, 10-12 Ekim 2019.

[17]. Travesset-Baro, O., Rosas-Casals, M., Jover, E., Transport Energy Consumption in Mountainous Roads, Transp. Res. Part D: Transp. Environ., 2015, 34: 16–26.

[18]. Fiori C, Ahn K, Rakha H. A. Power-Based Electric Vehicle Energy Consumption Model:

Model Development and Validation, Appl. Energy, 2016, 168: 257–268.
[19]. Wyatt, D. W., Li, H., Tate, J. E.,The impact of Road Grade on Carbon dioxide (CO_2) Emission of a Passenger Vehicle in Real-World Driving, Transp. Res. Part D: Transp. Environ., 2014, 32: 160–170.
[20]. Sun, X. H., Yamamoto, T., Morikawa, T., Stochastic Frontier Analysis of Excess Access to Mid-trip Battery Electric Vehicle Fast Charging. Transp. Res. Part D: Transp. Environ., 2015, 34: 83–94.
[21]. Liu, K., Yamamoto, T., Morikawa, T., Impact of Road Gradient on Energy Consumption of Electric Vehicles, Transportation Research Part D., 2017, 54(1): 74–81.
[22]. Mruzek, M., Gajdáč, I., Ľuboš, K., Barta, D., Analysis of Parameters Influencing Electric Vehicle Range, Procedia Engineering, 2016, 134: 165–174.
[23]. Aktaş, U., Abdallah, K., "Aerodynamics Concept Study of Electric Vehicles", Master's thesis, Sweden: Department of Applied Mechanics Division of Vehicle Engineering and Autonomous Systems Chalmers University of Technology Gothenburg, (2017).
[24]. Hucho, W. H., "Aerodynamics of Road Vehicles", 4 th edition, SAE International, Warrendale, PA, ISBN: 978-0-7680-0029-0, (1998).
[25]. Robinette, R. (2017), Mazda Miata CFD Generated Aerodynamic Info, <http://robrobinette.com/S2000Aerodynamics.htm>.
[26]. Palin, R., Johnston, V., Johnson, S., The Aerodynamic Development of the Tesla Model S - Part 1: Overview, SAE Int. doi:10.4271/2012-01-0177, (2012).
[27]. Littlewoodd, R, Passmore, M., The optimization of Roof Trailing Edge Geometry of a Simple Square-back, SAE Technical Paper, 2010-04-12.
[28]. Soares, R. F., De Souza, F. J., The Brazilian Automotive Scenario Over the Hatch 2015 Car Models: A view from Aerodynamics, SAE Technical Paper, 2015-36-0518.
[29]. Daryakenari, B., Abdullah, S., Zulkifli, R. (2013). Reducing Vehicle Drag Force through a Tapered Rear Side Wall, SAE Int. J. Commer. Veh., 2013, 6, 582-588. https://doi.org/10.4271/2013-01-9020.
[30]. Kumar, A., Singh, A., Regin, A. F., Study on Effect of Ground Clearance on Performance of Aerodynamic Drag Reduction Devices for Passenger Vehicle Using CFD Simulations, SAE Technical Paper, 2015-26-0197.
[31]. Ishihara, Y., Takagi, H., Asao, K., Aerodynamic Development of the New Developed Electric Vehicle, SAE Technical Paper, 2011-39-7230.
[32]. Sterken, L., Lofdahl, L., Sebben, S., Walker, T., Effect of Rear-end Extensions on the Aerodynamic Forces of an SUV, SAE Technical Paper, 2014-01-0602.
[33]. Kang, S., Cho, J., Jun, S., Park, H., Song, K., A Study of an Active Rear Diffuser Device for Aerodynamics Drag Reduction of Automobiles, SAE Technical Paper, 2012-01-0173.
[34]. Don, S. (2019). Dragqueens: aerodynamics compared. Car and Driver, <https://www.caranddriver.com/features/a15108689/drag-queens-aerodynamics-compared-comparison-test/>.
[35]. Owen, E. C., Steiber, J., Development of Auxiliary Power Units for Electric Hybrid vehicle, Southwest Research Institute San Antonio, Texas, (1997).

[36] Güneş, H., Design and Manufacture of Tube Type Nonhollow Linear Generators for Suspension Systems of Electric and Hybrid Cars, Proceedings of the Institution of Mechanical Engineers, Part E: Journal of Process Mechanical Engineering. March 2021. doi:10.1177/09544089211000016